Medical Physics
The International Journal of Medical Physics Research and Practice

A limited-angle intrafraction verification (LIVE) system for radiation therapy

Lei Ren, You Zhang, and Fang-Fang Yin

Citation: Medical Physics **41**, 020701 (2014); doi: 10.1118/1.4861820
View online: http://dx.doi.org/10.1118/1.4861820
View Table of Contents: http://scitation.aip.org/content/aapm/journal/medphys/41/2?ver=pdfcov
Published by the American Association of Physicists in Medicine

Medical Physics Letter

A limited-angle intrafraction verification (LIVE) system for radiation therapy

Lei Ren[a)]
Department of Radiation Oncology, Duke University Medical Center, DUMC Box 3295, Durham, North Carolina 27710 and Medical Physics Graduate Program, Duke University, 2424 Erwin Road, Suite 101, Durham, North Carolina 27705

You Zhang
Medical Physics Graduate Program, Duke University, 2424 Erwin Road, Suite 101, Durham, North Carolina 27705

Fang-Fang Yin
Department of Radiation Oncology, Duke University Medical Center, DUMC Box 3295, Durham, North Carolina 27710 and Medical Physics Graduate Program, Duke University, 2424 Erwin Road, Suite 101, Durham, North Carolina 27705

(Received 29 September 2013; revised 10 December 2013; accepted for publication 11 December 2013; published 23 January 2014)

Purpose: Currently, no 3D or 4D volumetric x-ray imaging techniques are available for intrafraction verification of target position during actual treatment delivery or in-between treatment beams, which is critical for stereotactic radiosurgery (SRS) and stereotactic body radiation therapy (SBRT) treatments. This study aims to develop a limited-angle intrafraction verification (LIVE) system to use prior information, deformation models, and limited angle kV-MV projections to verify target position intrafractionally.

Methods: The LIVE system acquires limited-angle kV projections simultaneously during arc treatment delivery or in-between static 3D/IMRT treatment beams as the gantry moves from one beam to the next. Orthogonal limited-angle MV projections are acquired from the beam's eye view (BEV) exit fluence of arc treatment beam or in-between static beams to provide additional anatomical information. MV projections are converted to kV projections using a linear conversion function. Patient prior planning CT at one phase is used as the prior information, and the on-board patient volume is considered as a deformation of the prior images. The deformation field is solved using the data fidelity constraint, a breathing motion model extracted from the planning 4D-CT based on principal component analysis (PCA) and a free-form deformation (FD) model. LIVE was evaluated using a 4D digital extended cardiac torso phantom (XCAT) and a CIRS 008A dynamic thoracic phantom. In the XCAT study, patient breathing pattern and tumor size changes were simulated from CT to treatment position. In the CIRS phantom study, the artificial target in the lung region experienced both size change and position shift from CT to treatment position. Varian Truebeam research mode was used to acquire kV and MV projections simultaneously during the delivery of a dynamic conformal arc plan. The reconstruction accuracy was evaluated by calculating the 3D volume percentage difference (VPD) and the center of mass (COM) difference of the tumor in the true on-board images and reconstructed images.

Results: In both simulation and phantom studies, LIVE achieved substantially better reconstruction accuracy than reconstruction using PCA or FD deformation model alone. In the XCAT study, the average VPD and COM differences among different patient scenarios for LIVE system using orthogonal 30° scan angles were 4.3% and 0.3 mm when using kV+BEV MV. Reducing scan angle to 15° increased the average VPD and COM differences to 15.1% and 1.7 mm. In the CIRS phantom study, the VPD and COM differences for the LIVE system using orthogonal 30° scan angles were 6.4% and 1.4 mm. Reducing scan angle to 15° increased the VPD and COM differences to 51.9% and 3.8 mm.

Conclusions: The LIVE system has the potential to substantially improve intrafraction target localization accuracy by providing volumetric verification of tumor position simultaneously during arc treatment delivery or in-between static treatment beams. With this improvement, LIVE opens up a

new avenue for margin reduction and dose escalation in both fractionated treatments and SRS and SBRT treatments. © *2014 American Association of Physicists in Medicine*. [http://dx.doi.org/10.1118/1.4861820]

Key words: Intrafraction verification, prior knowledge, PCA motion modeling, free form deformation, image reconstruction

1. INTRODUCTION

Modern radiation therapy technologies have enabled us to deliver highly conformal radiation dose to treat tumors with tight margin. In addition to pretreatment localization and verification, intrafraction verification is critical as intrafraction motion can potentially lead to under coverage of the tumor and overdose to healthy tissues. This is especially true for stereotactic radiosurgery (SRS) and stereotactic body radiation therapy (SBRT) treatments due to their tight planning target volume (PTV) margin,[1] high fractional dose, small fraction number, and long treatment time.[2]

Currently, on-board kV fluoro or MV cine images can be used for intrafraction target verification in 2D. However, the accuracy of target localization in the 2D images is often limited due to the overlay of other anatomical structures in the images, especially for small tumors treated in SBRT. Implanting markers in the tumor can improve the localization accuracy,[3] but this approach may not be applicable for all patients as it requires the invasive procedure of marker implantation. In addition, migration of the marker through the treatment course impairs the localization accuracy. Another major drawback of all 2D imaging techniques is that they do not provide 3D or 4D volumetric information of the target, which is critical for tumor localization especially when the tumor experiences both deformation and motion during the breathing cycle. Digital tomosynthesis (DTS) has been studied recently for verification of lung radiotherapy.[4] Similar as 2D images, DTS does not provide full volumetric information. 3D or 4D-CBCT are effective tools for pretreatment verification,[5] but they have limited applications for intrafraction verification because of their large scanning angle, long scanning time, high imaging dose, and mechanical constraints. Choi *et al.* developed a method to acquire kV projections during gated VMAT delivery to reconstruct patient on-treatment CBCT images for post-treatment evaluation.[6] The limitation of this technique is that it can only reconstruct CBCT images after the full arc delivery is completed, and therefore cannot verify and correct target positioning during treatment delivery. Li *et al.*[7,8] proposed to estimate lung tumor location from a single x-ray projection using lung motion models extracted from planning 4D-CT based on principal component analysis (PCA). Although the method has the potential to provide real time 3D tumor localization intrafractionally, its accuracy may be limited when patients have anatomical or breathing pattern changes from CT scan to treatments. Our group and several other groups have developed methods to use free form deformation (FD) model and prior knowledge to reconstruct 4D images based on limited projections.[9–11] However, results showed that these methods have limited accuracy when reconstructing using projections acquired within a limited scan angle. This is mainly due to the limited information in the limited angle projections and the large amount of variables in the FD model.

In this study, we propose a limited-angle intrafraction verification (LIVE) system for volumetric intrafraction target verification during arc treatment delivery or in-between static 3D/IMRT beams. Specifically, we focus on the development of LIVE for lung SBRT in this manuscript. LIVE acquires limited-angle kV projections simultaneously during arc treatment delivery or in-between static treatment beams as the gantry moves from one beam to the next. Orthogonal complementary limited-angle MV projections are acquired from the exit fluence of the arc treatment beam or in-between static beams to provide additional anatomical information. LIVE uses patient prior planning 4D-CT images as prior knowledge, and considers the on-board volumetric images to be reconstructed as a deformation of the prior images. LIVE solves the deformation field using both PCA and FD deformation models and the data fidelity constraint. The on-board images are then obtained by deforming the prior CT images based on the deformation field solved. The feasibility of the LIVE system was validated through simulation studies using the 4D digital extended-cardiac-torso (XCAT) phantom and phantom studies using the CIRS 008A dynamic thoracic phantom (Computerized Imaging Reference Systems, Norfolk, VA).

2. METHODS

2.A. Image acquisition scheme

The LIVE system aims to provide intrafraction verification during arc treatment delivery or in-between static 3D/IMRT beams. In our study, a dynamic conformal arc treatment plan was made to deliver conformal dose to the PTV. MV beam's eye view (BEV) cine images and orthogonal kV images were simulated or acquired during the arc treatment delivery. Limited angle kV and MV projections were retrospectively selected for reconstruction of volumetric images of the target. Different scanning angles (15° and 30°) and scanning directions were used for image reconstruction to evaluate their effects on the reconstruction accuracy.

2.B. Conversion between kV and MV projection images

Previously we developed a linear fitting technique to aggregate kV and MV projections.[12] One pair of kV and BEV MV projections of the patient is acquired at the same gantry angle before the treatment. The same BEV region is extracted

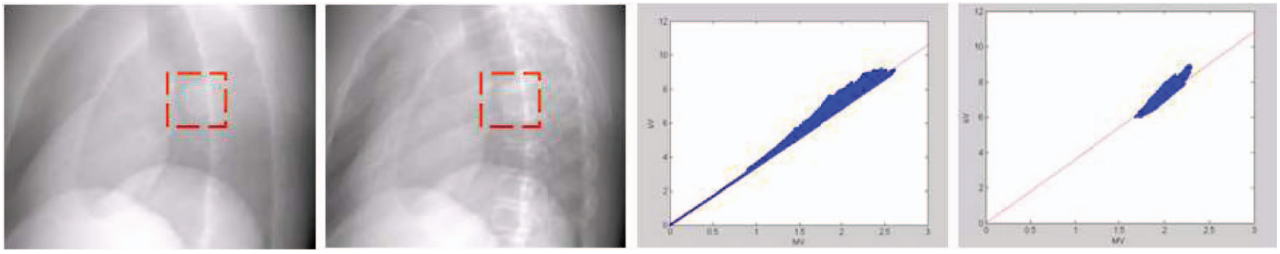

FIG. 1. Linear fitting between pixel values in the kV and MV projection images.

from the kV and MV images after blank scan correction and −log transformation. A linear function is fitted between pixel values in kV and MV projections, as shown in Fig. 1. The MV projections acquired from the actual treatment beam will be converted to kV projection using the fitted linear function.

2.C. Reconstruction techniques

2.C.1. Prior knowledge based reconstruction

As shown in Fig. 2, one phase of patient planning 4D-CT is used as the prior images I_{prior}. The on-board image volume I_{new} at one phase is considered as a deformation of the prior image. To solve the deformation field, the data fidelity constraint can be used which requires the DRRs of I_{new} to match with the limited angle kV and MV projections acquired. The formula of the data fidelity constraint is shown as follows:

$$P^* I_{\text{new}}(I_{\text{prior}}, D) = \text{On board projections}, \quad (1)$$

where P is cone-beam projection matrix to describe the x-ray projection measurements. In reality, Eq. (1) may not be satisfied when planning CT is used as I_{prior} due to the gray level difference between planning CT and on-board CBCT. To solve this problem, the LIVE system uses normalized cross correlation (NCC)[13] as the metric for data fidelity constraint instead. Equation (1) is then substituted by the following equation:

$$\text{NCC}(P^* I_{\text{new}}(I_{\text{prior}}, D), \text{ On board projections}) = 1. \quad (2)$$

Once the deformation field D is solved, and the on-board images I_{new} at one phase are obtained by deforming the prior image I_{prior} based on D. This reconstruction can be repeated for each phase to obtain on-board 4D images. As the LIVE system only acquires limited angle kV and MV projections, Eq. (2) is an ill-posed problem without enough equations to solve the large number of variables in the deformation field D.[9,10] Here we introduce additional deformation models to reduce the number of variables and adding additional constraints to solve the problem.

2.C.2. Motion modeling based on principal component analysis

The PCA based motion modeling method builds major patient respiratory deformation modes from 4D-CT, and express the on-board deformation field to be solved as a linear combination of these deformation modes. Specifically, deformation fields are generated by performing deformable registration between the phase image selected as I_{prior} in Eq. (2) and all other phases of the 4D-CT. PCA analysis is then used to extract major deformation modes from all the deformation fields generated. In our method, the first three principal deformation modes are used as they are maximally decorrelated and proved to be sufficient in depicting lung motion.[7] The deformation field D to be solved in Eq. (2) is represented as a linear combination of the three principal deformation modes assuming that the breathing pattern does not change. The problem of solving the deformation field D is now converted into solving only three coefficients of the deformation modes, which substantially reduces the degree of freedom in the optimization. A gradient descent method is used as the optimizer to solve the coefficients by minimizing −NCC in Eq. (2).

Although PCA based method is efficient in solving the deformation field, its accuracy is highly dependent on the accuracy of the motion model extracted from 4D-CT. Patient anatomical and breathing pattern change from CT simulation to treatment will impair the accuracy of the PCA model, and therefore reduce the accuracy of the reconstruction.

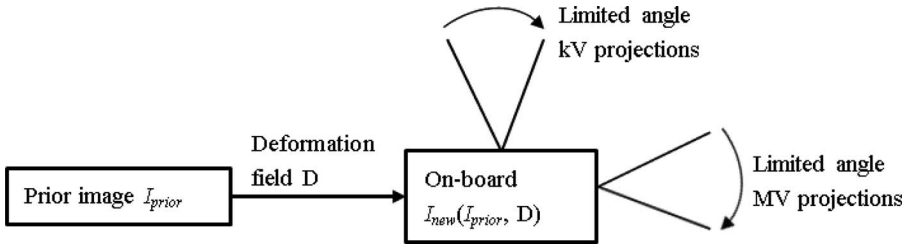

FIG. 2. Diagram of the prior knowledge based image reconstruction technique.

2.C.3. Free form deformation model

To improve accuracy of the PCA based method, a FD model is introduced in the reconstruction of LIVE system. In the FD model, each voxel has its own deformation field. To maintain the smoothness of the deformation field, the FD method minimizes the field deformation energy $E(D)$ defined by Lu *et al.*[14] during reconstruction. The deformation field is determined by solving the following constrained optimization problem:

$$D = \text{argmin}_{\forall D}\left(E\left(D\right)\right) \tag{3}$$

subject to the data fidelity constraint in Eq. (2).

An optimization algorithm similar as the ASD-POCS algorithm developed by Sidky *et al.*[15] is used to solve this problem. The deformation energy minimization and data fidelity constraint are enforced consecutively through gradient descent optimization with adaptive control of the step size of the deformation energy minimization to reach final convergence. Note that the FD based method is not based on any assumption about patient motion model. Therefore, this method is not affected by patient anatomical and breathing pattern changes from CT scan to treatment. However, FD based method is less efficient than PCA based method, and is prone to converge at local minimum values due to the large number of variables in the method.

2.C.4. Combining PCA and FD based methods in LIVE

As shown in Fig. 3, the LIVE system uses the PCA based method first to obtain a quick coarse estimation of the deformation field, and then uses the FD based method to further fine tune the deformation field. Given a much better starting point from the PCA based method, FD based method is able to reach the final results much faster without being stuck at local minimum values. On the other hand, adding FD based method after PCA based method can substantially reduce the errors of PCA based method caused by patient anatomy and breathing pattern changes from CT simulation to treatment.

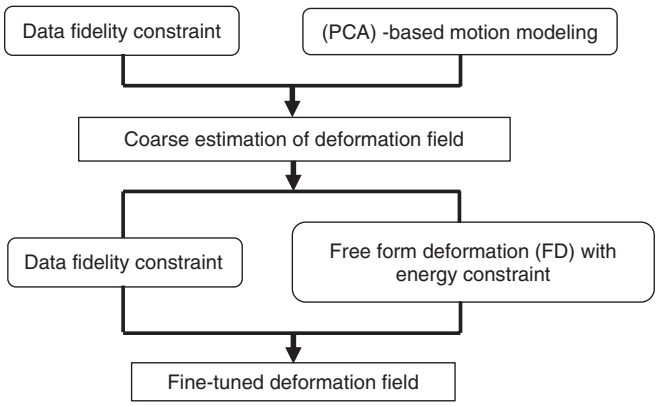

FIG. 3. Flowchart of the reconstruction algorithm of LIVE system.

2.D. Evaluation methods

2.D.1. XCAT simulation

XCAT is a digital anthropomorphic phantom developed based on the human anatomical database from the National Library of Medicine.[16] XCAT uses nonuniform rational B-spline surfaces to model highly realistic and detailed human anatomical structures. It can be utilized to generate 4D images according to anatomical parameters and respiratory profiles specified by the user. In our study, XCAT was first used to simulate patient 4D-CT images with a spherical tumor of 3 cm diameter inserted into the lung. The respiratory motion trajectory was sinusoidal with 4 s cycle. The peak-to-peak respiratory motion amplitudes for tumor and body were both 3 cm along superior-inferior (SI) direction and 2 cm in anterior-posterior (AP) direction. The end expiration phase of the 4D-CT was used as the prior image volume. Patient anatomical and breathing pattern changes were simulated in the on-board image volume for the following eight scenarios:

(1) both tumor and body motion amplitudes changed to 2 and 1.2 cm along SI and AP directions, respectively;
(2) tumor size shrunk to 2.5 cm in diameter and motion amplitude changes in (1);
(3) tumor size expanded to 4 cm in diameter and motion amplitude changes in (1);
(4) tumor average motion position shifted by 0.8 cm along SI direction, and motion amplitude changes in (1);
(5) tumor average motion position shifted by 0.8 cm along AP direction, and motion amplitude changes in (1);
(6) tumor average motion position shifted by 0.5 cm along SI, AP, and lateral directions, and motion amplitude changes in (1);
(7) 72° (20%) relative phase shift between tumor and body respiratory motion, and motion amplitude changes in (1);
(8) body motion amplitudes were changed to 2 and 1.2 cm along SI and AP directions, and tumor motion amplitudes were changed to 4 and 3 cm along SI and AP directions, respectively.

Two monochromatic energies were used to generate on-board image volumes: 40 keV to simulate on-board kV imaging and 1 MeV to simulate on-board MV imaging. Full fan on-board kV projections were simulated by Siddon's ray-tracing techniques based on the keV imaging volume, and both BEV and full MV projections were simulated based on the MeV imaging volume. The new on-board image volume was reconstructed by the LIVE system using the prior 4D-CT images and simulated on-board kV-MV projections. The tumor volume in the simulated on-board image volume was used as the ground truth.

2.D.2. CIRS phantom study

The CIRS 008A dynamic thoracic phantom is an anthropomorphic lung phantom, which represents an average human thorax in composition and proportion. A lung equivalent rod containing a spherical target is inserted into the lung

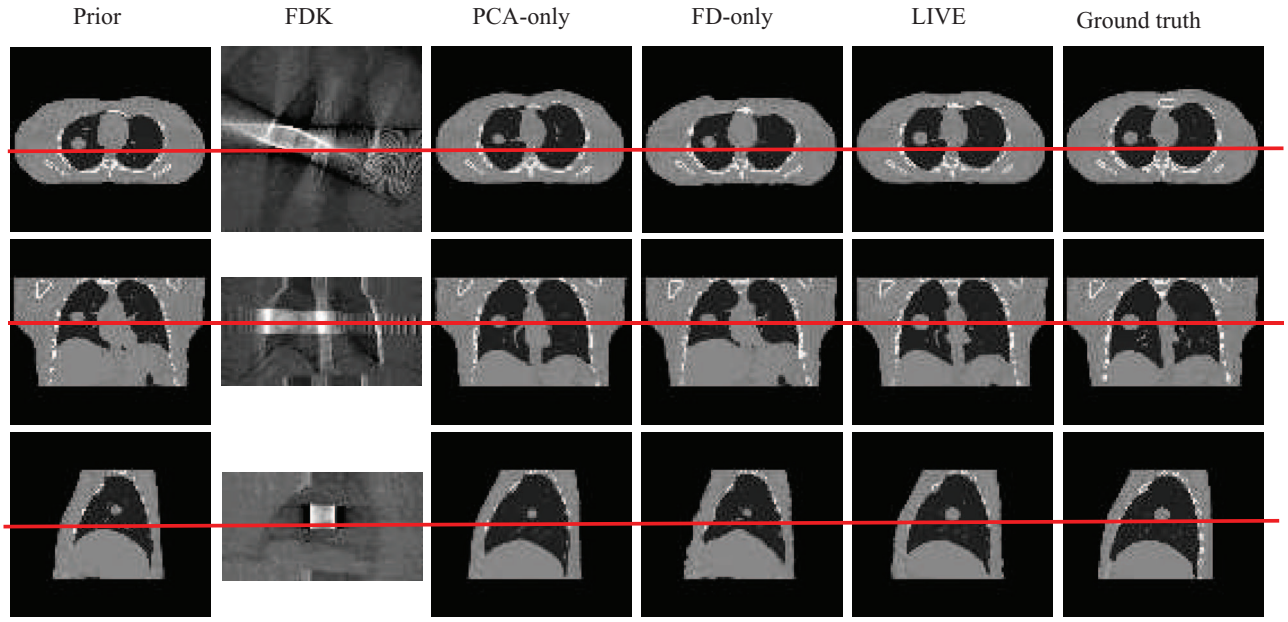

FIG. 4. Comparison between images reconstructed by different methods using orthogonal 30° kV and BEV MV projections in scenario (6) of the XCAT study.

equivalent lobe of the phantom. The rod can be driven by a motion actuator moving the target along the SI direction according to a respiratory motion profile specified by the user. In our experiments, 4D-CT scans were acquired on a GE (GE Healthcare, Waukesha, WI) LightSpeed RT scanner with 120 kVp, 260 mAs. A target of 3 cm diameter was programmed to move in the lung at 4 s period and 3 cm peak-to-peak amplitude sinusoidally during the 4D-CT scan. Internal target volume (ITV) was contoured based on the maximum intensity projection (MIP) images of the 4D-CT, and PTV was generated by expanding the ITV by 5 mm. A dynamic conformal arc plan was made in Eclipse using 6 MV beam to deliver 12 Gy × 4 to the PTV. The MLC aperture in the plan was generated by adding a 5 mm margin to the PTV. Truebeam (Varian Medical Systems, Palo Alto, CA) research mode was used for treatment delivery and simultaneous kV-MV acquisition. The MLC positions were exported from the plan made in Eclipse and used for specifying the MLC locations in the xml file used for research mode delivery. The MV acquisition was realized by enabling MV cine ("Continuous" mode, ∼1.15 MU per projection) acquisition during treatment. The kV acquisition was realized by enabling intermittent kV projection ("DynamicGain" mode, 120 kVp, 80 mA, 25 ms, full-fan) acquisition every 1° during the treatment delivery. The treatment delivery time was 3 min. A target of 2 cm diameter was inserted in the lung instead for the on-board treatment position to simulate tumor shrinkage in patients. The end inspiration phase of the 4D-CT was used as the prior image, and the on-board images were reconstructed for one representative respiratory phase by the LIVE system. The target in the lung experienced both size change (from 3 to 2 cm in diameter) and a centroid location shift of 1 cm from CT scan to on-board treatment position. To isolate the motion artifacts from reconstruction accuracy evaluation, the on-board target is fixed at the position corresponding to the specific respiratory phase to be reconstructed during the on-board scan. A 200° full-fan CBCT scan was acquired separately to be used as the ground truth.

2.D.3. Evaluation metrics

Two metrics were used for reconstruction accuracy evaluation: volume percentage difference (VPD) and center of mass shift (COMS). VPD is defined by the following formula:

$$\mathrm{VPD} = \frac{|V \cup V_0 - V \cap V_0|}{V_0} * 100\%, \tag{4}$$

where V and V_0 are the contoured target 3D volume in the estimated and ground truth images. The COMS is defined by the following formula:

$$\mathrm{COMS} = \sqrt{\Delta x^2 + \Delta y^2 + \Delta z^2}, \tag{5}$$

where Δx, Δy, Δz are center-of-mass distances between V and V_0 along each of the three canonical directions. Reconstruction accuracy of the LIVE system for both 15° and 30° scanning angles were evaluated. Unless otherwise mentioned, the 30° scan angle was from 240°–270° for kV and 330°–0° for orthogonal MV imaging. The 15° scan has the same central gantry angle as the 30° scan.

3. RESULTS

3.A. XCAT simulation

Figure 4 shows the results for different reconstruction techniques using orthogonal 30° kV and BEV MV projections in patient scenario (6) of the XCAT simulation. The projection angular sampling interval was 0.6° for both kV and MV imaging. As shown in the figure, the LIVE system achieved better reconstruction accuracy than PCA-only and FD-only methods in reconstructing the tumor volume. The

TABLE I. Average VPD and COMS of eight patient scenarios simulated by XCAT in Sec. 2.D.1 for different reconstruction techniques using orthogonal kV and BEV MV projections.

	PCA-only		FD-only		LIVE	
	Ortho 15°	Ortho 30°	Ortho 15°	Ortho 30°	Ortho 15°	Ortho 30°
VPD	61.6%	55.4%	96.4%	85.5%	15.1%	4.3%
COMS (mm)	5.6	4.9	13.9	11.6	1.7	0.3

Feldkamp-Davis-Kress (FDK) reconstruction method had severe distortion artifacts due to the limited angle projections used. Table I shows the average VPD and COMS of the eight patient scenarios described in Sec. 2.D.1 for different reconstruction techniques using kV and BEV MV projections acquired within different scanning angles. Both the VPD and COMS were computed for the reconstruction of end-inspiration phase of on-board imaging volume. For comparison, we also evaluated the reconstruction accuracy using kV and open field MV projections, which can be acquired during gantry rotation in-between 3D/IMRT beams. The results of average VPD and COMS are shown in Table II.

3.B. CIRS phantom study

Figure 5 shows the linear fitting results between pixel values of acquired kV and MV projections for the CIRS phantom. The two projections were acquired prior to the treatment delivery to establish a linear relationship between the kV and MV projections. 1 MU was used for the MV imaging. Figure 5(c) shows that the kV and MV pixel values are linearly correlated. Figure 5(d) shows an example of the raw MV cine image acquired during arc treatment delivery. Note that Figs. 5(a) and 5(b) are the projections after blank scan normalization and −log transformation, while Fig. 5(d) is the original raw image without any processing. Figure 6 shows the results for different reconstruction techniques using orthogonal 30° kV and BEV MV projections acquired in the CIRS phantom study. The projection sampling frequency was 1 per degree for both kV and MV imaging. The target size was changed from 3 to 2 cm in diameter, and target location had 1 cm shift. LIVE system achieved the best reconstruction accuracy among all the reconstruction techniques. Table III shows the VPD and COMS for different techniques and scanning angles. The reconstruction accuracy of LIVE was also evaluated for different scanning directions, as the results shown in Table IV.

4. DISCUSSION

Note that the results shown above are reconstruction of tumor volume at one respiratory phase. Results showed that increasing scanning angle improves the reconstruction accuracy. Scanning direction does not have significant effects that on the reconstruction accuracy. The number of projections N can be acquired for each phase over certain gantry rotation angle α is dependent on the gantry rotation speed ω and patient breathing cycle T. The relationship is as follows:

$$N = \frac{\alpha/\omega}{T}. \tag{6}$$

For example, in a typical dynamic conformal arc plan with 45°–60° wedge, the MU needed to deliver 12 Gy per fraction is around 4000 MU for 120° arc angle. If we use the 600 MU/min dose rate, the gantry rotation speed during arc delivery will be around: $\omega = \frac{120^\circ}{\frac{4000\ \text{MU}}{600\ \text{MU/min}}} = 0.3^\circ/\text{s}$. Then for a 15° arc segment, the total delivery time will be 15°/0.3°/s = 50s, which covers around 12 breathing cycles for a 4 s cycle. This means we can acquire around 12 projections over the 15° angle for each respiratory phase. For higher fractional dose scheme, such as 18 Gy/fraction, the gantry rotation speed will be slower to deliver higher MU, which allows acquiring more projections for each phase. For faster arc delivery such as VMAT, the rotation speed ω will be faster with less number of projections N acquired for each phase, which may affect the reconstruction accuracy of the LIVE system. We can potentially mitigate this problem by increasing the scanning angle α in Eq. (6). Note that the above discussions are all for free breathing treatments. For respiratory-gated treatments, Eq. (6) still holds except that T needs to be changed to T^* which is the gating duty cycle. For example, if 3 out of 10 phases are selected as gating window, then $T^* = \frac{3}{10}T$, and $N^* = \frac{10}{3}N$ mean the number of projections acquired in the gated treatment is 10/3 times the number of projections acquired in the free-breathing treatment given the same gantry rotation angle and rotation speed. As a result, LIVE is less affected by the

TABLE II. Average VPD and COMS of eight patient scenarios simulated by XCAT in Sec. 2.D.1 for different reconstruction techniques using orthogonal kV and open field MV projections.

	PCA-only		FD-only		LIVE	
	Ortho 15°	Ortho 30°	Ortho 15°	Ortho 30°	Ortho 15°	Ortho 30°
VPD	59.1%	59.6%	89.6%	65.9%	10.1%	4.5%
COMS (mm)	5.0	5.0	11.6	8.5	1.2	0.3

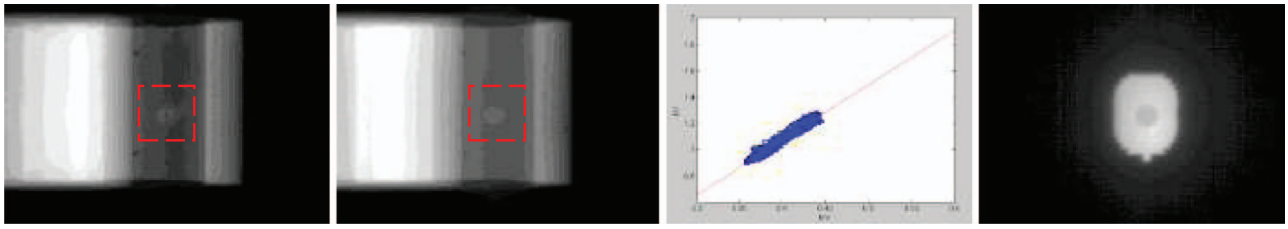

(a) (b) (c) (d)

FIG. 5. Linear fitting between pixel values in the kV and MV projection images for the CIRS phantom. (a) Pretreatment KV image. (b) Pretreatment MV image. (c) Linear fitting between pixel values in ROI of pretreatment kV-MV images. (d) MV cine image acquired during treatment delivery.

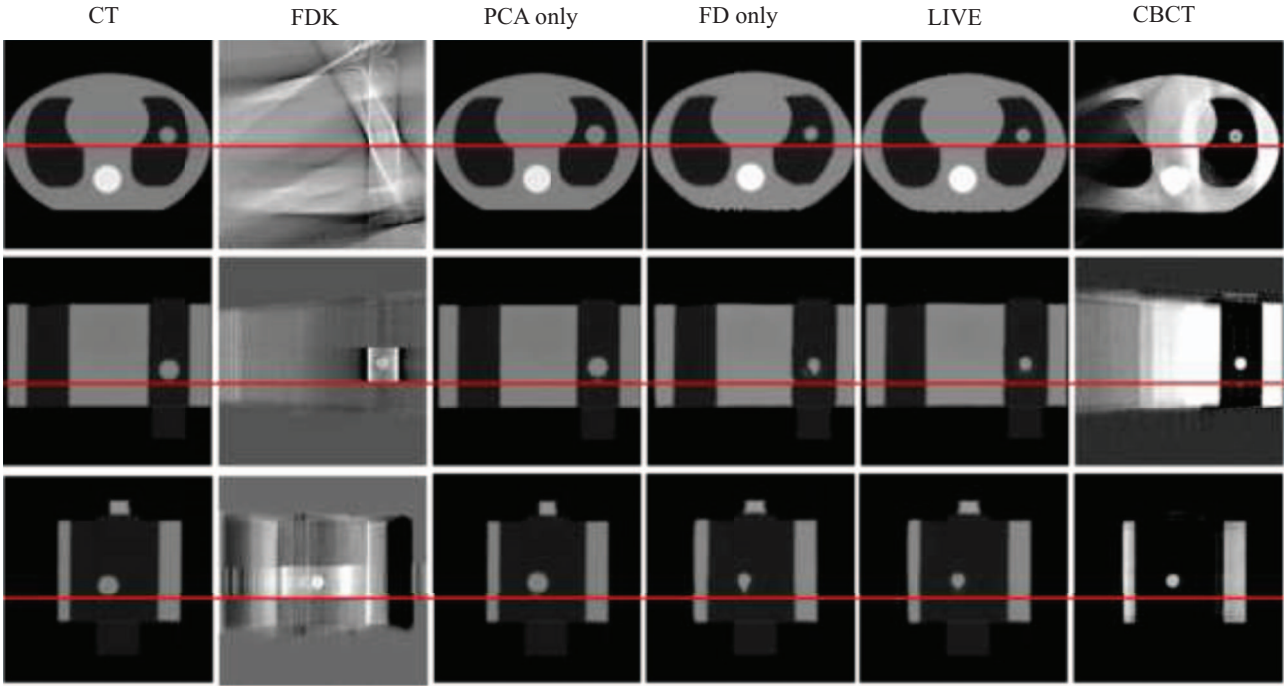

FIG. 6. Comparison between images reconstructed by different methods using orthogonal 30° kV and BEV MV projections in the CIRS phantom study.

TABLE III. VPD and COMS for different reconstruction techniques using orthogonal kV and BEV MV projections acquired for a CIRS phantom.

	PCA-only		FD-only		LIVE	
	Ortho 15°	Ortho 30°	Ortho 15°	Ortho 30°	Ortho 15°	Ortho 30°
VPD	233.1%	232.6%	82.5%	27.6%	51.9%	6.4%
COMS (mm)	5.6	3.0	5.6	1.9	3.8	1.4

TABLE IV. VPD and COMS for LIVE reconstruction using orthogonal kV and BEV MV projections acquired along different scanning directions in the CIRS phantom study.

Scanning directions	kV: 240°–270° MV: 330°–0°	kV: 270°–300° MV: 0°–30°	kV: 300°–330° MV: 30°–60°	kV: 330°–0° MV: 60°–90°	kV: 0°–30° MV: 90°–120°
VPD	6.4%	6.7%	2.8%	6.2%	3.5%
COMS (mm)	1.4	1.1	0.8	1.2	0.9

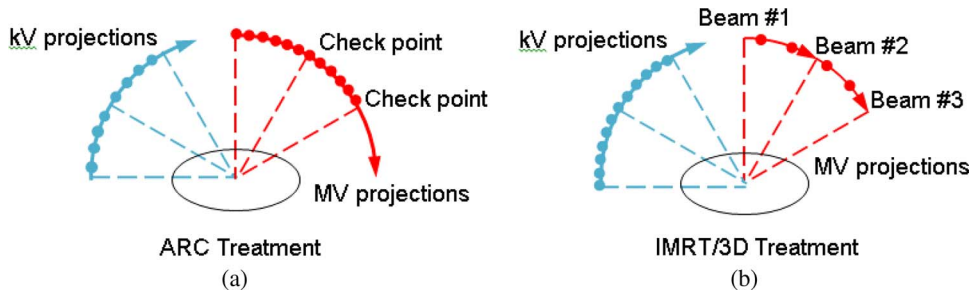

FIG. 7. Image acquisition scheme of the LIVE system for different types of treatments. (a) ARC treatment and (b) IMRT/3D treatment. Dots in the kV/MV acquisition arcs indicate the projection sampling frequency for different scenarios.

fast gantry rotation speed in VMAT for gated treatments. For breath-hold treatments, as the tumor remains almost static, there is no need for 4D reconstruction. The number of projections that can be acquired for 3D reconstruction is

$$N = \frac{\propto}{\omega} \times f, \tag{7}$$

where f is the image acquisition frame rates. The maximum gantry rotation speed ω allowed for a Linac is 6°/s. Imaging frame rates f for both MV cine and kV fluoro are above 10 fps. For a gantry rotation angle α of 30°, according to Eq. (7), over 50 projections can be acquired even for the fastest gantry rotation speed possible, which are adequate for reconstruction based on our previous study. Therefore, the fast gantry rotation speed of VMAT would not be an issue for the LIVE system for breath-hold treatments.

In clinical practice, the LIVE system can be implemented through different acquisition schemes for different types of treatments: (1) In an arc treatment, limited-angle BEV MV projections will be densely acquired from the exit fluence of the treatment beam with no extra MV imaging dose introduced. Orthogonal kV projections will be acquired sparsely during the arc delivery to obtain additional anatomical information, as shown in Fig. 7(a).The arc treatments reaches a checkpoint after certain gantry rotation angle where the LIVE system generates volumetric images based on the most recent limited angle kV-MV projections to verify target position. If the target is within the PTV, the arc treatment continues until reaching the next checkpoint. Otherwise, the treatment stops to correct the target misalignment. Note that as the tumor may be partially blocked by leaves in a VMAT treatment, there will be less information available in the MV cine images. As a result, more kV projections may need to be acquired to account for the loss of information in MV images. (2) In IMRT/3D treatments, the LIVE system acquires both kV and MV projections as the gantry moves from one beam to the next, as shown in Fig. 7(b). Unlike in arc treatments, the MV imaging dose here is extra dose to the patient, and needs to be minimized. Therefore, MV projections can be acquired more sparsely and kV projections can be acquired more densely during the gantry rotation. The LIVE system will primarily rely on kV projections for image reconstruction.

The LIVE system will be the first volumetric x-ray imaging technique to verify target position in 3D/4D during arc treatment delivery or during gantry rotation in-between 3D/IMRT beams. The LIVE system has the potential to significantly improve intrafraction target localization accuracy for SBRT treatments. The intrafraction images from LIVE are also more accurate than interfraction CBCT images for dose delivery estimation in adaptive radiation therapy as they are more reflective of actual patient position during treatment. With these improvements, LIVE opens up a new avenue for margin reduction and dose escalation in lung SBRT. The basic idea of LIVE system is also applicable for intrafraction verification for treatments of other clinical sites, including brain, spine, liver, prostate, and breast.

This study is mainly to provide a proof-of-concept and verify the feasibility of the LIVE system in reconstructing full volumetric images using limited-angle kV-MV projections. The next step is to improve the efficiency of the system to make it applicable for clinical usage. The LIVE system can be accelerated in the following approaches: (1) Multiresolution scheme, parallel computing, and hardware acceleration. Similar as typical registration algorithms, multiresolution scheme can be used for deformation field searching in LIVE to increase its efficiency and robustness. Parallel computing and hardware acceleration using the computer graphics card also have great potential to improve the speed of the algorithm. (2) Uneven acquisition and reconstruction strategy. To minimize the extra time required for reconstruction, LIVE can start reconstruction as soon as the first few kV-MV projections have been acquired at the beginning of the limited angle. The deformation field is then iteratively fine-tuned as more projections are acquired within the scan angle. To obtain a better starting point of the deformation field, projections can be more densely sampled at the beginning of the limited angle and less sampled as it gets closer to the end of the limited angle. This strategy will maximize the use of acquisition time for simultaneous reconstruction.

The linear fitting used for kV-MV conversion is an approximation approach. A more accurate approach is the dual CT technique, as shown in Fig. 8. In this technique, the kV planning CT is converted to MV planning CT at the same energy as the treatment beam using Monte Carlo (MC) simulation prior to treatment. Then LIVE uses both kV CT and MV CT as prior information, and deforms kV CT and MV CT to match their DRRs with on-board kV and MV projections, respectively. The reconstruction algorithm solves the deformation field by minimizing the data fidelity constraints from both kV and MV projections. The dual-CT technique is

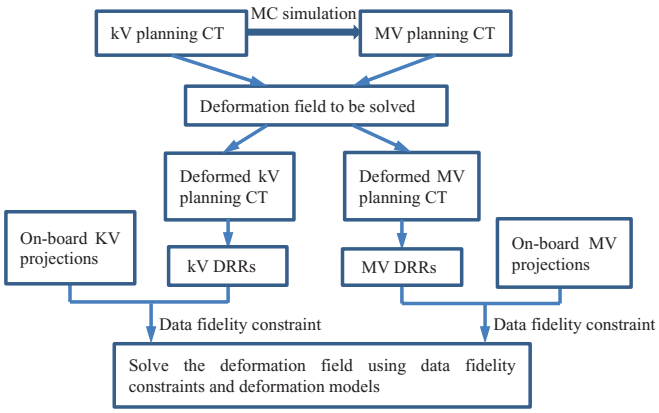

FIG. 8. Flow chart of the dual-CT technique.

theoretically more accurate than the linear fitting technique as it does not require the assumption about the linear conversion between kV and MV projections. This technique will be investigated in the future study.

5. CONCLUSION

We have developed a LIVE system to reconstruct volumetric images using limited angle kV and MV projections for intrafraction verification. Preliminary validation showed that LIVE can reconstruct target volume accurately using projections acquired within a 30° scanning angle during arc treatment delivery or during gantry rotation in-between 3D/IMRT beams. LIVE can potentially reduce the treatment errors caused by intrafraction motion for both fractionated and SRS/SBRT treatments to allow further margin reduction and dose escalation.

ACKNOWLEDGMENTS

This work was partially supported by a research grant from Varian Medical Systems. The authors also would like to thank Dr. Paul Segars for use of his XCAT program.

[a]Author to whom correspondence should be addressed. Electronic mail: lei.ren@duke.edu; Telephone: 919-668-0489; Fax: 919-681-7183.

[1]W. Li, T. G. Purdie, M. Taremi, S. Fung, A. Brade, B. C. Cho, A. Hope, A. Sun, D. A. Jaffray, A. Bezjak, and J. P. Bissonnette, "Effect of immobilization and performance status on intrafraction motion for stereotactic lung radiotherapy: analysis of 133 patients," Int. J. Radiat. Oncol., Biol., Phys. **81**, 1568–1575 (2011).

[2]T. G. Purdie, J. P. Bissonnette, K. Franks, A. Bezjak, D. Payne, F. Sie, M. B. Sharpe, and D. A. Jaffray, "Cone-beam computed tomography for on-line image guidance of lung stereotactic radiotherapy: localization, verification, and intrafraction tumor position," Int. J. Radiat. Oncol., Biol., Phys. **68**, 243–252 (2007).

[3]B. Cho, P. R. Poulsen, A. Sawant, D. Ruan, and P. J. Keall, "Real-time target position estimation using stereoscopic kilovoltage/megavoltage imaging and external respiratory monitoring for dynamic multileaf collimator tracking," Int. J. Radiat. Oncol., Biol., Phys. **79**, 269–278 (2011).

[4]J. R. van Sornsen de Koste, M. Dahele, H. Mostafavi, S. Senan, L. van der Weide, B. J. Slotman, and W. F. Verbakel, "Digital tomosynthesis (DTS) for verification of target position in early stage lung cancer patients," Med. Phys. **40**, 091904 (11pp.) (2013).

[5]D. A. Jaffray and J. H. Siewerdsen, "Cone-beam computed tomography with a flat-panel imager: initial performance characterization," Med. Phys. **27**, 1311–1323 (2000).

[6]K. Choi, L. Xing, A. Koong, and R. Li, "First study of on-treatment volumetric imaging during respiratory gated VMAT," Med. Phys. **40**, 040701 (4pp.) (2013).

[7]R. Li, J. H. Lewis, X. Jia, T. Zhao, W. Liu, S. Wuenschel, J. Lamb, D. Yang, D. A. Low, and S. B. Jiang, "On a PCA-based lung motion model," Phys. Med. Biol. **56**, 6009–6030 (2011).

[8]R. Li, X. Jia, J. H. Lewis, X. Gu, M. Folkerts, C. Men, and S. B. Jiang, "Real-time volumetric image reconstruction and 3D tumor localization based on a single x-ray projection image for lung cancer radiotherapy," Med. Phys. **37**, 2822–2826 (2010).

[9]L. Ren, J. Zhang, D. Thongphiew, D. J. Godfrey, Q. J. Wu, S. M. Zhou, and F. F. Yin, "A novel digital tomosynthesis (DTS) reconstruction method using a deformation field map," Med. Phys. **35**, 3110–3115 (2008).

[10]L. Ren, I. J. Chetty, J. Zhang, J. Y. Jin, Q. J. Wu, H. Yan, D. M. Brizel, W. R. Lee, B. Movsas, and F. F. Yin, "Development and clinical evaluation of a three-dimensional cone-beam computed tomography estimation method using a deformation field map," Int. J. Radiat. Oncol., Biol., Phys. **82**, 1584–1593 (2012).

[11]J. Wang and X. Gu, "High-quality four-dimensional cone-beam CT by deforming prior images," Phys. Med. Biol. **58**, 231–246 (2013).

[12]F. F. Yin, H. Guan, and W. Lu, "A technique for on-board CT reconstruction using both kilovoltage and megavoltage beam projections for 3D treatment verification," Med. Phys. **32**, 2819–2826 (2005).

[13]J. Dang, L. Ouyang, X. Gu, and J. Wang, "Deformation vector fields (DVF)-driven image reconstruction for 4D-CBCT," Med. Phys. **40**, 457 (2013).

[14]W. Lu, M. L. Chen, G. H. Olivera, K. J. Ruchala, and T. R. Mackie, "Fast free-form deformable registration via calculus of variations," Phys. Med. Biol. **49**, 3067–3087 (2004).

[15]E. Y. Sidky and X. Pan, "Image reconstruction in circular cone-beam computed tomography by constrained, total-variation minimization," Phys. Med. Biol. **53**, 4777–4807 (2008).

[16]W. P. Segars, M. Mahesh, T. J. Beck, E. C. Frey, and B. M. Tsui, "Realistic CT simulation using the 4D XCAT phantom," Med. Phys. **35**, 3800–3808 (2008).